

Moisture transport in paper passing through the fuser nip of a laser printer

Seungjun Lee · Gil Ho Yoon

Received: 25 November 2016 / Accepted: 20 May 2017 / Published online: 5 June 2017
© Springer Science+Business Media Dordrecht 2017

Abstract Paper curls in printers should be prevented since they cause paper jams and degradation of printing quality. Moisture transport due to high temperature in the fuser nip of a printer is one of main reasons for paper curls. In order to predict and control the paper curls, it is therefore essential to understand the mechanisms of heat and moisture transport in paper. In this paper, we derived a coupled heat and moisture transport model and applied it to the situation where a paper sheet moves between two rollers having different temperatures in a fuser nip. A series of simulations were carried out with varying parameters related to the characteristics of printer paper, the environment, and paper/environment interfaces. The simulation results provided a deep understanding of the moisture transport mechanisms and identified several key variables affecting changes of moisture profiles as a function of time. The time-dependent moisture contents data will be fed into a mechanical model to obtain the quantitative amount of the nip curl.

Keywords Moisture transport · Paper curl · Porous medium · Printer

Introduction

Curling of paper in copy machines or printers is a problematic phenomenon since it causes paper jams, low quality of prints, and reduction in the stackable limit at the output tray. The sources of the paper curls can be categorized into three groups, as shown in Fig. 1: high temperature and high pressure at the fusing nip (*nip curl*), severely curved paths (*path curl*), and contraction due to drying toner on the surface (*contraction curl*). Particularly, the nip curl occurring in a fuser is assumed to contribute mainly to the total size of the curl. In the fusing process, paper passes through a nip between a heat roller and a pressure roller. Since the temperature inside the nip is typically controlled on the side of the heat roller, the top and bottom surfaces of the paper are exposed to different temperatures. The difference in temperature results in moisture transport within the paper, generating moisture gradients across the paper. The variation of the moisture contents causes local expansion or shrinkage of fibers, creating mechanical deformations such as curls in the paper (Larsson and Wågberg 2010; Lipponen et al. 2008). Therefore, the moisture transport process coupled by heat transport needs to be understood in order to predict and control the paper curls in printers.

S. Lee
Department of Mechanical, Robotics, and Energy
Engineering, Dongguk University, Seoul, Korea

G. H. Yoon (✉)
School of Mechanical Engineering, Hanyang University,
Seoul, Korea
e-mail: ghy@hanyang.ac.kr

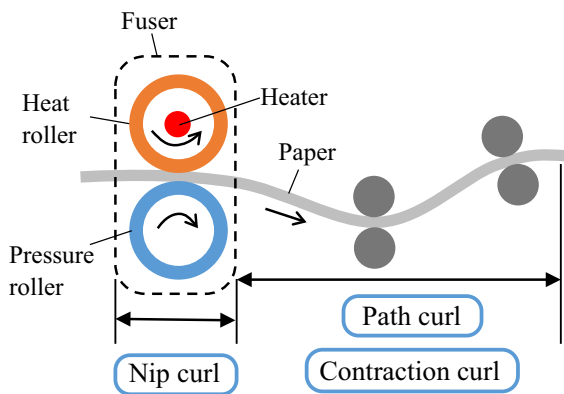


Fig. 1 Schematic of mechanisms of typical paper curls in printers

Moisture transport in cellulose-based materials used in food, textiles, and packaging industries has been recently of interest. For example, moisture content affects the insulation properties of fabric materials (Fan and Wen 2002; Huang et al. 2007); it can change the physical properties of packaging materials, damaging the inner contents such as food, cosmetics and pharmaceuticals (Bedane et al. 2016, 2014). The effect of moisture on physical and mechanical properties of paper has received considerable interest from many researchers (Haslach 2000; Menart et al. 2011). The combined effect of moisture and temperature on the mechanical properties of paper was studied systematically by a tensile test method (Linville and Östlund 2014; Salmen and Back 1980). The directional mechanical properties of paper were measured at different moisture contents and the reason was suggested due to different fiber orientations (Coffin et al. 2004). Humidity cycling has been shown to accelerate creep in paper due to the moisture-gradient-driven stress concentration (Habeger and Coffin 2000; Habeger et al. 2001). In addition, it has been reported that the plastic strain of paper is significantly affected by moisture contents (Land et al. 2010). For engineering applications, the moisture and temperature dependent mechanical model was proposed and successfully applied to the paper forming process (Linville and Östlund 2016).

A theoretical model of moisture transport in paper has been suggested by Bandyopadhyay et al. (Bandyopadhyay et al. 2000, 2002). The model was derived from a two-equation model of generalized transport in a porous medium (Sáez et al. 1989). In their study, the

paper was modeled as a porous medium consisting of two phases of fibers and pores. Using the mathematical model, moisture transport in a paperboard stack was described when the surfaces of the paper stack were exposed to differential humidity. The two-phase model has been widely used to describe the parallel diffusion of water in the pore and fiber phase of paper (Bedane et al. 2016; Gupta and Chatterjee 2003a, b; Leisen et al. 2002; Ramarao et al. 2003). Using the model, the moisture transmission rate and moisture distributions of a paper stack were calculated and the theoretical calculations were validated by experiment. Although these models described well the moisture transport and change in moisture contents in paper caused by exposure to humidity differential conditions, they are limited to use in isothermal conditions. Because the mathematical model does not consider the thermal effect on moisture transport, it is not suitable for application in paper curl simulations in the printing process, since the paper is exposed to large changes in temperature. Recently, Zapata et al. developed a theoretical model that considers both heat and moisture transport in printer paper (Marin Zapata et al. 2013). The mathematical model was used to study the transient temperature and moisture profiles of a paper sheet moving on one side of a heated metal surface.

In this paper, we studied moisture transport in a paper sheet passing through the fusing nip of a printer using a coupled heat and moisture transport model. The purpose of the study is to establish a theoretical framework that can predict paper curls in printers. In the fuser, the paper is exposed to high temperatures between two rollers for a short period of time. In the study, the situations are described according to the boundary conditions of two hot surfaces. The moisture transport process was numerically solved as a function of time with finite element procedures. We investigated the effects of various parameters and environmental conditions of humidity and temperatures on changes in moisture contents. The study provides an in-depth understanding of the fundamental mechanisms of the moisture transport process in a paper sheet inside a printer and enables identification of the dominant parameters affecting significantly the moisture profile. The data for the evolution of the moisture profile will be fed into a mechanical model to calculate the nip curl in the future. This paper is structured as follows. First, the theoretical framework for the moisture and heat transport is described. Then, the

boundary conditions for the simulation of the nip curl are explained. The simulation results with various parameters and conditions are then shown and discussed. Finally, the conclusions are given at the end.

Mathematical model

The moisture transport and heat coupled model has been well derived in the reference (Marin Zapata et al. 2013). Our theoretical framework was established mainly on the base of the model suggested by Marin Zapata et al. (2013), and the boundary conditions that describe the practical printing situation were applied for our study. The mathematical model is summarized in this section, and our simulation model with the boundary conditions is described in the next section.

We considered a representative elementary volume (REV) of a paper sheet to model the mass transport of moisture as shown in Fig. 2. Since paper is a porous medium composed of cellulose fibers, the REV of paper consists of two domains: cellulose fibers (gray) and a pore space (white). The moisture can be desorbed from the fibers when the temperature or humidity in the pores changes. The desorbed moisture transports by diffusion through the pore space. Diffusion through the fibers is negligible since the diffusivity in fibers is considerably lower than that in pores. As the humidity in the pores changes due to the transported moisture, the moisture can again be absorbed into the fiber.

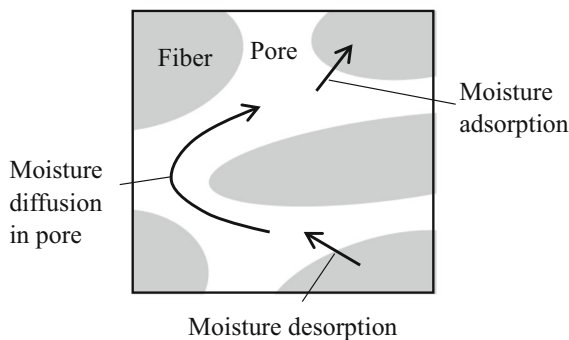


Fig. 2 Representative element volume (REV) inside a paper sheet consisting of two phases (gray: fiber and white: pore). The moisture travels through pores and is absorbed or desorbed into fibers

These mechanisms of mass transport can be expressed by the following partial differential equations. The fiber matrix is denoted by the right subscript ‘*f*’ and the pore space is denoted by the right subscript ‘*p*’. The time-dependent moisture concentration at each domain is described as:

$$(1 - \eta) \frac{\partial c_f}{\partial t} = S, \quad (1)$$

$$\eta \frac{\partial c_p}{\partial t} = \eta \nabla \cdot (D \nabla c_p) - S, \quad (2)$$

where η is the ratio of the pore volume, c_f is the moisture concentration in the fibers [kg m^{-3}], t is time [s], c_p is the moisture concentration in the pores [kg m^{-3}], D is the diffusivity of moisture in the pores [$\text{m}^2 \text{s}^{-1}$], and S is a source term that represents the absorption/desorption rate of the moisture from the pores to the fibers per unit volume. The term S is positive for absorption to the fibers and negative for desorption since the supply of moisture is considered in terms of the fiber. In addition, the sign of the term S in Eqs. (1) and (2) should be opposite because the mass of the exchanged moisture is conserved.

As the difference between the equilibrated water concentration and present water concentration increases, more of the moisture in the pore space tends to be absorbed into the fibers. Therefore, the source term S can be described by a linear relation of the unbalanced moisture concentrations:

$$S = k(c_f^{eq} - c_f), \quad (3)$$

where k is the mass transport coefficient [s^{-1}] and c_f^{eq} is the equilibrated moisture concentration in the fibers [kg m^{-3}]. Since the moisture concentrations in the fiber and those near the pore are the same at the equilibrium state, c_f^{eq} is related to c_p . This relation can be derived from the moisture sorption isotherm, which represents the relationship between the moisture content in a material and humidity at equilibrium. The Guggenheim, Andersen and de Boer (GAB) equation is well known for determining the isotherm of paper (Parker et al. 2006; Quirijns et al. 2005):

$$M^{eq} = \frac{M_0 C K H_R}{(1 - K H_R)(1 - K H_R + C K H_R)}, \quad (4)$$

where M^{eq} is the ratio of moisture content to a dry material at equilibrium [-]. M_0 , C , and K are the GAB

parameters and H_R is the relative humidity [–]. The GAB parameters are typically obtained by fitting the curves, which are determined by the sorption isotherm experiment. When M^{eq} is determined at a given humidity and temperature, the moisture content in the fiber at equilibrium can be calculated, assuming the contribution by the pore is relatively low:

$$c_f^{eq} = \rho_f M^{eq}. \quad (5)$$

The relative humidity H_R in Eq. (4) is defined as:

$$H_R = \frac{c_p}{c_p^s}, \quad (6)$$

where c_p^s is the saturated moisture concentration in air. From the ideal gas law, c_p^s can be calculated by

$$c_p^s = \frac{P^s}{RT}, \quad (7)$$

where P^s is the saturation vapor pressure, R is the gas constant ($461 \text{ J K}^{-1} \text{ kg}^{-1}$), and T is temperature [K]. P^s can be calculated by the Arden-Buck's relation (Buck 1981). We used the parameters of the e_{w6} curve for higher temperature intervals in the literature (Buck 1981):

$$P^s = 6.1121 \exp \left[\left(18.564 - \frac{T}{254.4} \right) \left(\frac{T}{T + 255.57} \right) \right], \quad (8)$$

where T is in Celsius and P^s is in millibars. From Eqs. (7) and (8), the temperature dependent c_p^s is summarized as

$$c_p^s = \frac{A_1}{T} \exp \left(\frac{A_2 T^2 + A_3 T + A_4}{T + A_5} \right), \quad (9)$$

where T is in Kelvin and the constants from A_1 to A_5 are given by $A_1 = 1.3258 \text{ [K]}$, $A_2 = -0.003931 \text{ [K}^{-1}\text{]}$, $A_3 = 20.7115 \text{ [–]}$, $A_4 = -5364.05 \text{ [K]}$, and $A_5 = -17.58 \text{ [K]}$.

The time-dependent temperature T [K] in the paper sheet is determined by the heat equation derived from the conservation of energy:

$$c\rho \frac{\partial T}{\partial t} = \nabla \cdot (\lambda \nabla T) + (1 - \eta)h \frac{\partial c_f}{\partial t}, \quad (10)$$

where c is the specific heat of paper [$\text{J kg}^{-1} \text{ K}^{-1}$], ρ is the density of paper [kg m^{-3}], λ is the thermal conductivity of paper [$\text{J m}^{-1} \text{ K}^{-1} \text{ s}^{-1}$], and h is the

heat of sorption of moisture [J kg^{-1}]. The last term is a heat source associated with the adsorption/desorption of moisture (Marin Zapata et al. 2013). When the water molecules transfer from the fiber to the pore ($\partial c_f / \partial t < 0$), the temperature is expected to decrease.

Simulation model

Figure 3 shows a schematic of a paper sheet that passes through a fusing nip in a printer. In the fusing nip, the paper moves between the heat roller and the pressure roller. A high temperature above 100°C is supplied to the heat roller for printing. The temperature of the pressure roller is lower than that of the heat roller since the temperature is controlled only at the heat roller. A one-dimensional mathematical model is constructed to simulate the moisture transport in the paper sheet because the curl of the paper mainly occurs due to the moisture transport along the thickness of the paper. The axis is set along the thickness of the paper sheet where the origin of the x axis is located at the bottom of the paper. The thickness of the paper is assumed to be $110 \text{ }\mu\text{m}$. Thus, the top of the paper is at $x = L = 110 \text{ }\mu\text{m}$. The one-dimensional mathematical model can be rewritten as:

$$(1 - \eta) \frac{\partial c_f}{\partial t} = k(c_f^{eq} - c_f), \quad (11)$$

$$\eta \frac{\partial c_p}{\partial t} = \eta D \frac{\partial^2 c_p}{\partial x^2} - k(c_f^{eq} - c_f), \quad (12)$$

$$c\rho \frac{\partial T}{\partial t} = \lambda \frac{\partial^2 T}{\partial x^2} + (1 - \eta)h \frac{\partial c_f}{\partial t}. \quad (13)$$

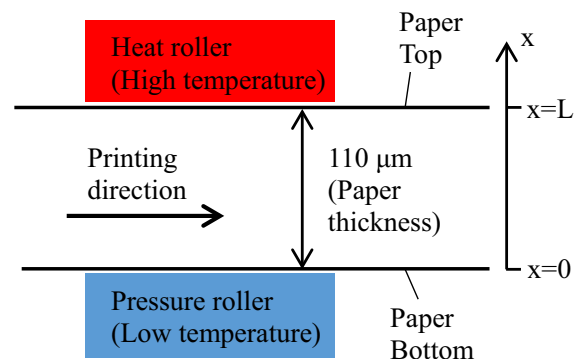


Fig. 3 Schematic showing a simulation system of a paper sheet moving through a fusing nip in a printer

In our transient finite element simulations, the paper sheet is inside the nip at $0 < t < t_1$ and out of the nip at $t_1 < t < t_2$. Therefore, the boundary conditions are modeled time-dependently. For the moisture concentration at the fiber (c_f), the fluxes at the top and bottom surfaces are always zero since we assumed that the moisture is only transported by the pores so it is emitted only through the pores. For the moisture concentration at the pore (c_p), the fluxes at the top and bottom surfaces are zeros when the paper is inside the nip since both the top and bottom surface of the paper are blocked by the rollers. After the paper exits the nip, the surfaces of the paper will be exposed to the environment so the flux conditions are subjected to be changed. Accordingly, the boundary conditions for the variable c_p are summarized as follows:

$$x = 0; \quad 0 < t < t_1; \quad D \frac{\partial c_p}{\partial x} = 0, \quad (14a)$$

$$x = L; \quad 0 < t < t_1; \quad D \frac{\partial c_p}{\partial x} = 0, \quad (14b)$$

$$x = 0; \quad t_1 < t < t_2; \quad D \frac{\partial c_p}{\partial x} = K_m(c_p - c_p^{env}), \quad (14c)$$

$$x = L; \quad t_1 < t < t_2; \quad D \frac{\partial c_p}{\partial x} = K_m(c_p^{env} - c_p), \quad (14d)$$

where K_m is the convective mass transfer coefficient on the surface of the paper and c_p^{env} is the moisture concentration in the environment. For the temperature, the top surface comes into contact with the heat roller and the bottom surface comes into contact with the pressure roller when the paper is inside the nip. When the paper is outside the nip, both surfaces will be exposed to the temperature of the environment. Therefore, the boundary conditions for the temperature are summarized as follows:

$$x = 0; \quad 0 < t < t_1; \quad \lambda \frac{\partial T}{\partial x} = K_h^{roller}(T - T^{pr}), \quad (15a)$$

$$x = L; \quad 0 < t < t_1; \quad \lambda \frac{\partial T}{\partial x} = K_h^{roller}(T^{hr} - T), \quad (15b)$$

$$x = 0; \quad t_1 < t < t_2; \quad \lambda \frac{\partial T}{\partial x} = K_h^{air}(T - T^{env}), \quad (15c)$$

$$x = L; \quad t_1 < t < t_2; \quad \lambda \frac{\partial T}{\partial x} = K_h^{air}(T^{env} - T), \quad (15d)$$

where K_h^{roller} is the thermal conductance between the roller and the paper, K_h^{air} is the heat transfer coefficient between air and the paper, T^{pr} is the temperature of the pressure roller, T^{hr} is the temperature of the heat roller, and T^{env} is the temperature of the environment.

Results

Before we perform our simulations, we tested the mathematical model for reliability. The model was applied to the situation in the reference (Leisen et al. 2002) where the paper is placed between two different humidity. In the reference, the evolution of the moisture distribution in the thickness direction of paper was measured by magnetic resonance imaging (MRI). For the test, the boundary conditions of the model were modified to describe that the paper is exposed to air during the entire simulation. The humidity was set to 100% on the bottom side and 0% on the top side. The initial moisture contents in the fiber and pore were set to zero. The same parameters were used from the reference. The calculated moisture profiles in Fig. 4 show a good trend with the experimental data of the unsymmetrical distribution, indicating that the model has a reliable capability to describe the moisture evolution inside paper according to environmental conditions.

To our best knowledge, the material properties of paper are not homogeneous and they are difficult to determine. We therefore began our simulations based on the parameters in the reference (Marin Zapata et al. 2013). In the reference, the major parameters such as the mass transport coefficient, diffusivity, porosity, and thermal conductance were determined by experiments for commercial printing papers. Therefore, simulations with these parameters will provide useful results for practical applications of the model to real printing situations. After that, we performed a series of simulations with varying the parameters to see the effect of variations on the results. The parameters should depend on the kinds of papers and printing machines. The parameters for various kinds of papers will be measured by experiments in future. The parameters used in the simulation are summarized in Table 1; these values are used unless mentioned otherwise. The temperature of the heat roller is set as 170 °C and the temperature of

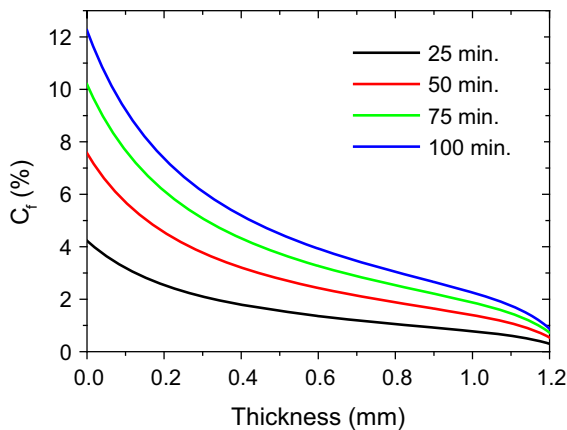


Fig. 4 Evolution of the moisture profile during the moisture ingress from the bottom of the paper

Table 1 Parameters used in simulations

Parameter	Value
η	0.47
k	0.0035 s^{-1}
D	$3 \times 10^{-6} \text{ m}^2 \text{ s}^{-1}$
c	$1200 \text{ J kg}^{-1} \text{ K}^{-1}$
ρ	818 kg m^{-3}
ρ_f	1500 kg m^{-3}
λ	$0.51 \text{ W m}^{-1} \text{ K}^{-1}$
h	$2.5 \times 10^6 \text{ J kg}^{-1}$
K_m	0.011 m s^{-1}
K_h^{roller}	$1180 \text{ W m}^{-2} \text{ K}^{-1}$
K_h^{air}	$11.48 \text{ W m}^{-2} \text{ K}^{-1}$

the pressure roller is set as 100°C . The environment temperature is set as 30°C and the relative humidity is set at 85%. It is assumed that the paper is in equilibrium before printing. Therefore, the initial moisture concentration in fiber is determined by Eqs. (4)–(9) and the initial c_f is calculated as 12.3134%. The GAB parameters are assumed to be constant as $M_0 = 0.0329$, $K = 0.865$, and $C = 39.09$ (Marin Zapata et al. 2013).

Figure 5a shows the temperature evolution of the paper. At the start of simulation, the temperature of the paper increases rapidly due to the supply of heat from both ends of the paper where they contact the hot rollers. At $t = 0.1 \text{ s}$, the temperature of the paper reaches approximately 120°C with a gentle

gradient along the thickness direction. The gradient of temperature is due to the difference in temperature of the rollers. The level of the gradient depends on the value of the thermal conductivity λ in Eq. (13). With a smaller λ , the temperature gradient will be larger. After $t = 0.1 \text{ s}$, the paper exits the nip and the temperature of the paper gradually decreases since it is exposed to the environment temperature.

Figure 5b shows the evolution of the moisture contents in the pore. The value of c_p increases when the paper is inside the nip and decreases when it is outside of the nip. The increase of c_p is due to the desorption of moisture from the fibers since no flux exists at the boundaries when the paper is inside the nip. The moisture in the pore began to evacuate to air when the paper is outside of the nip, resulting in reducing the concentrations around both ends at $t = 0.11 \text{ s}$.

The value of c_f in Fig. 5c slowly decreases when the paper is inside the nip. Although the decrease of the concentration accelerates after the paper exits the nip, the total amount of reduction is less than 0.1% and no gradient along the thickness is observed. The moisture desorption from the fibers is caused by the change of the equilibrium moisture concentration due to the change in temperature.

Figure 5d shows the decrease of the equilibrium moisture content. As the temperature increases, the saturated moisture concentration increases according to Eq. (9), leading to a decrease of the relative humidity in the pore. Then, the value of M^{eq} decreases, whereby desorption occurs since the right hand side in Eq. (11) becomes negative. In Fig. 5d, M^{eq} decreases by almost half, from 12 to 6% in a short period of time of 0.005 s. This rapid change of the equilibrium moisture concentration due to the high temperature increase inside the nip is the fundamental cause of the changes in the moisture concentration. Therefore, the exact isotherm relation of paper, which defines the equilibrium moisture contents, is important for the precise prediction of moisture transport in the paper. In this study, we used the constant GAB parameters, although they are known to depend on temperature. Although the constant GAB parameters are used, our simulations can successfully show meaningful changes in a qualitative sense. The temperature-dependent GAB parameters will be determined by experiment in future work.

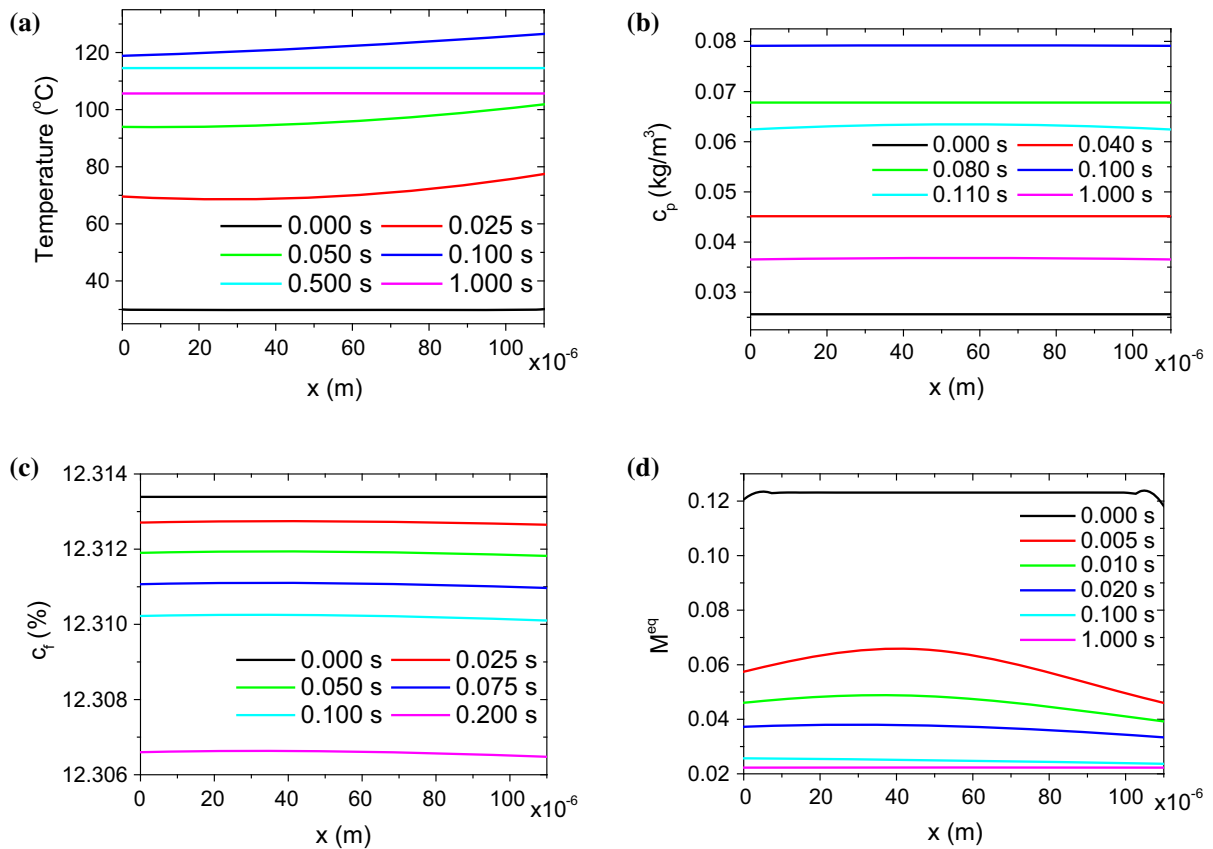


Fig. 5 Simulation results showing variance of profiles along the thickness of the paper as a function of time: **a** temperature inside the paper, **b** moisture contents in the pores, **c** moisture

contents in the fibers, and **d** ratio of the equilibrium moisture content in the fibers to the moisture content in dry paper

Since paper curls in printers are known to occur due to the differential moisture concentrations, the change of the moisture contents shown in Fig. 5c is not sufficiently significant to show curls. We changed the value of the mass transport coefficient k in Eq. (11). The increase of k will lead to the increase of the reacting speed of moisture absorption/desorption between the fibers and pores upon temperature changes. Figure 6 shows the moisture profiles with the 100 and 1000 times higher k values than the parameter in Table 1. As the value of k is higher, the gradient of the moisture contents increases. Therefore, the difference of moisture contents at the ends increases. The difference is calculated approximately as 0.15% with $k = 0.35$ and 1% with $k = 3.5$. For $k = 3.5$, the moisture content decreases at the high temperature region and increases at the low temperature region, showing a clear moisture transport

phenomenon from high to low temperature regions. The value of $k = 3.5$ will be used continuously in all of the later simulations. In the simulation, the mass transport coefficient k is found to play a significant role in generating a large gradient of the moisture contents. However, the available value of the coefficient in references shows a wide range of 0.003–2.83 (Bandyopadhyay et al. 2000; Bedane et al. 2016). The mass transport coefficient k represents how fast moistures are absorbed or desorbed from fibers to pores. Since this exchange occurs at the molecular level, it is difficult to measure the value directly by experiment. In the sense, atomic simulations may be useful to determine the coefficient and we plan to find the value by molecular dynamics simulations.

The effect of the moisture diffusion speed is studied by varying the diffusion coefficient. Figure 7a shows the moisture profiles at $t = 0.1$ with different values of

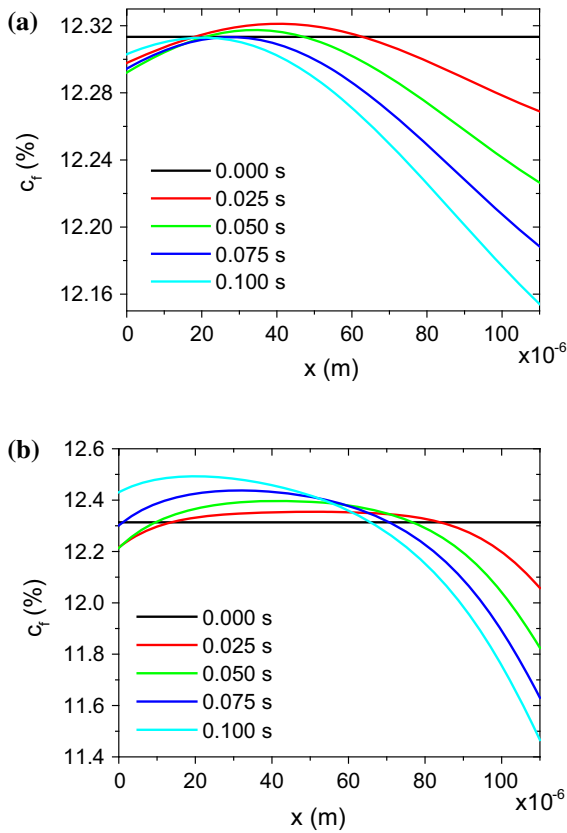


Fig. 6 Evolution of moisture profiles calculated with different mass transport coefficient values: **a** $k = 0.35$ and **b** $k = 3.5$

the diffusivity in the fibers (the black curve is the moisture content at $t = 0$). As the moisture diffusivity increases, the difference of moisture contents at both ends becomes large. When the diffusivity increases 10 times more than the parameter in Table 1, the difference of the moisture content in the fibers at the ends increases to 1.6%. This is because the larger diffusivity accelerates the moisture transport from high to low moisture contents, which flattens the gradient of the moisture content in the pores, as shown in Fig. 7b. The flat profile of the moisture content in the pores enables faster moisture adsorption/desorption according to the change in temperature. For example, at the high temperature region, the moisture content in the pore increases due to desorption. Then, the moisture desorption becomes decelerated because the relative humidity increases. However, if the desorbed moisture from the fibers transports quickly to other regions, the deceleration of the moisture desorption will be prevented, leading to large differential moisture contents.

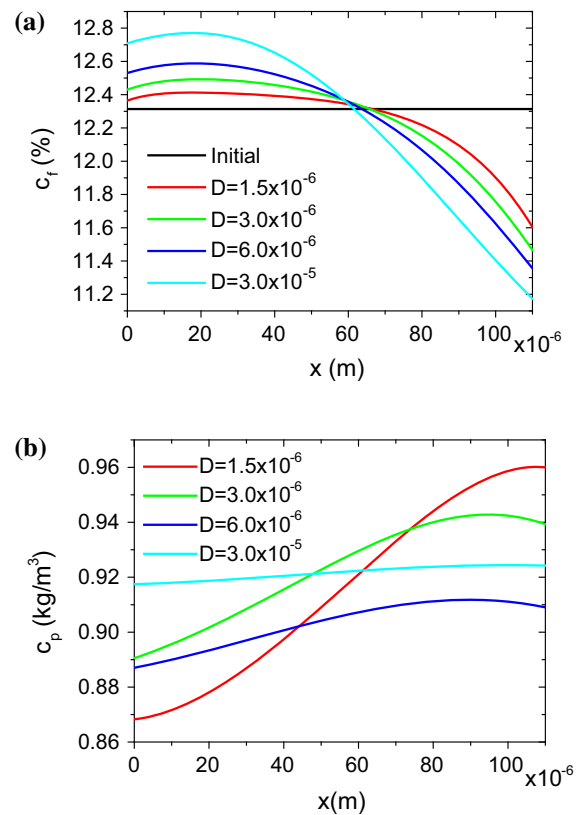


Fig. 7 Evolution of moisture profiles in **a** fibers and **b** pores calculated with different values of diffusivity

It should be noted that moisture induces swelling, particularly in the out-of-plane direction. If swelling is restrained inside the nip, the porosity will decrease, leading to the reduction in the moisture transport properties. This effect can be included by modeling the diffusion coefficient as a function of moisture contents. Although this effect is not considered in our model, the simulation results with varying the diffusivity and porosity will help to predict the swelling effect indirectly.

We studied the effect of the porosity in the paper. Figure 8a shows the moisture profiles at $t = 0.1$ with different porosity values of η . As the porosity increases, the difference of the moisture content increases: 0.6% at $\eta = 0.2$, 0.9% at $\eta = 0.4$, 1.1% at $\eta = 0.6$, and 1.3% at $\eta = 0.8$. This is because moisture in the pores can diffuse more quickly as the porosity increases, which has a similar effect to that of the higher diffusivity.

Next, the effect of thermal conductance between the paper and rollers is investigated. Figure 8b shows

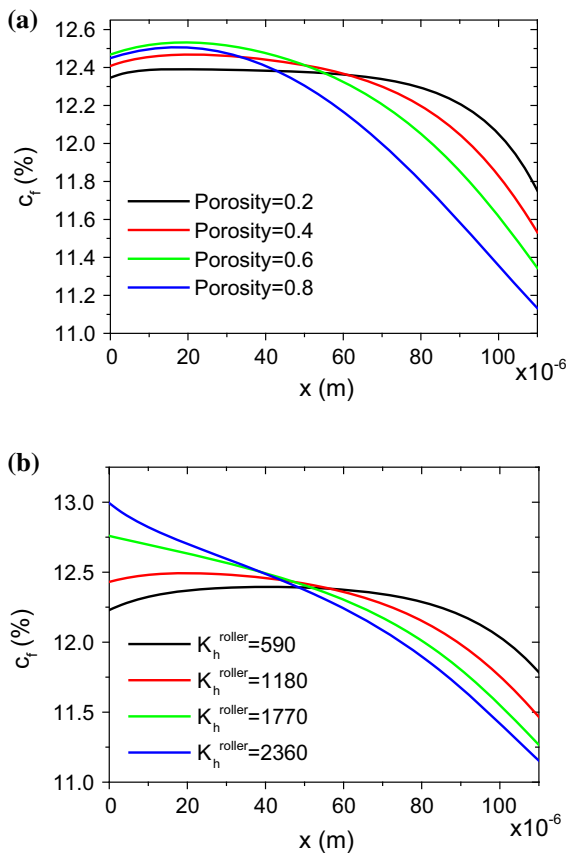


Fig. 8 Moisture profile at $t = 0.1$ s with different **a** porosity and **b** thermal conductance values between the rollers and paper

the moisture profiles at $t = 0.1$ with change in the values of thermal conductance. As the conductance increases, the gradient of the profile increases and the difference in the moisture content at both ends increases. When the value of the thermal conductance changes by 0.5, 1.5, and 2 times the parameter in Table 1, the difference is calculated as 0.45, 1.5 and 2%, respectively, showing an increase of approximately 0.5%. The higher conductance represents a better supply of heat from the roller, which enlarges the gradient of temperature in the paper, leading to a larger gradient of the moisture profile. This result demonstrates that paper curls can increase as the applied pressure between the rollers increases since it has been reported that the thermal conductance increases as the pressure increases (Noboa and Seyed-Yagoobi 2001).

The calculated moisture profiles can be related to the curl prediction using the laminate theory (Carlsson

1981). In the reference, the curvature of the laminate composed of multiple layers with different mechanical and expansional properties was calculated by the laminate theory. The theory has been reversely used to determine the expansion coefficient from the curved laminate due to moisture (Neagu et al. 2005). This theory can be used for our system since the mechanical strains along the thickness direction are induced by the different moisture contents instead of the different material properties. However, the direct application of the theory may not be allowed since viscoelastic nature of paper can play a significant role in our system. The curl in the printing process is not produced immediately upon the moisture transport. The curl is restrained inside the nip and begins to be generated after the paper is released out of the nip. Furthermore, the mechanical boundary conditions need to be properly considered for the restrained and released situations. The complete framework that can predict the curvature of paper will be developed by incorporating the mechanical model with the moisture transport model. In the following section, we focus on the difference of the moisture contents at two ends points, which represents two surfaces of paper, since the curvature can be calculated from strains due to moistures of two points in analogy to the bending of a bimetallic strip.

We studied the effect of environmental conditions such as relative humidity and temperature. Representative results are shown in Fig. 9. In Fig. 9, the curves represent the difference of the moisture contents at both surfaces as a function of time. A larger difference in the moisture contents will generate a larger curl. Figure 9a shows the simulation results with various relative humidity at 30 °C and Fig. 9b shows the results with various temperatures at a relative humidity of 85%. The overall trends of the curves are similar; when the paper is inside the nip ($0 < t < 0.1$), the difference of the moisture contents sharply increases due to the moisture transport. After the paper exits the nip, the difference decreases since the moisture in both ends of the paper evaporates into the air. The decrease in the moisture difference indicates that a larger amount of moisture escapes from the low temperature region (the moisture content is larger) than the high temperature region. As shown in Figs. 9a, b, the effect of relative humidity is larger than that of temperature. The calculated values of the maximum differences are summarized in Table 2. The average values at each relative humidity increase

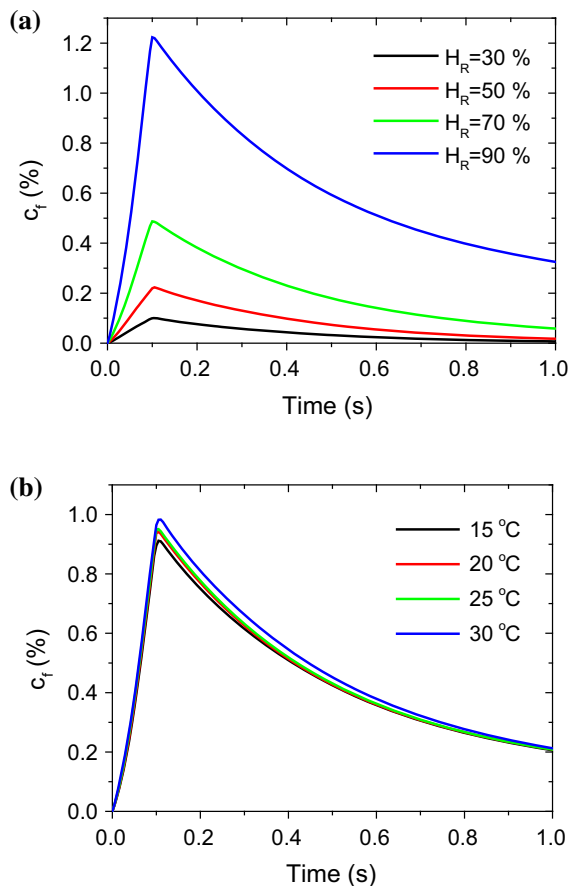


Fig. 9 Variance of the difference of the moisture contents at two ends as a function of time with different **a** relative humidity at 30 °C and **b** environment temperature at relative humidity of 85%

Table 2 Maximum difference of the moisture content between the surfaces

Environment temperature	Relative humidity			
	30%	50%	70%	90%
15 °C	0.0977%	0.2120%	0.4675%	1.1557%
20 °C	0.0983%	0.2136%	0.4781%	1.1714%
25 °C	0.0992%	0.2165%	0.4889%	1.2265%
30 °C	0.1003%	0.2194%	0.4873%	1.2232%
Average	0.0989%	0.2154%	0.4805%	1.1942%

almost exponentially as the relative humidity increases, indicating that the environmental humidity significantly affects the size of curls.

Lastly, we studied the effect of temperature of the rollers. Two variables were considered: the

temperature of the heat roller and the temperature difference between the two rollers. The calculated maximum moisture difference at the ends ($x = 0$ and $x = 110 \mu\text{m}$) are summarized in Table 3. The simulations were performed with an environment temperature of 30 °C and a relative humidity of 85%. As the temperature difference increases, the moisture difference tends to increase, which will lead to larger curls. However, the effect of the temperature of the heat roller is not clearly observed. For example, when the temperature of the heat roller increases from 170 to 200 °C, the moisture difference slightly decreases for the two different cases in which the temperature difference between the rollers is 50 and 65 °C, respectively.

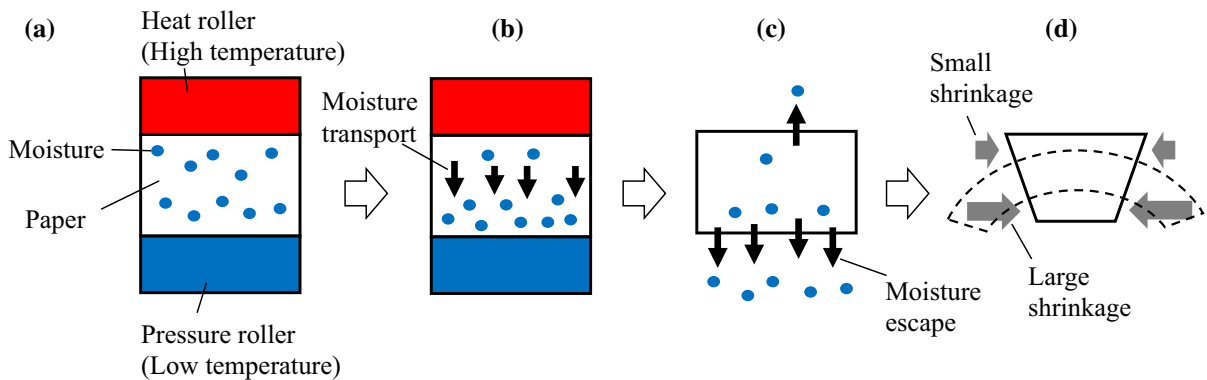
However, it is important to carefully consider whether the tendency for the moisture difference is related to the size of curls. It is typically agreed that a larger moisture difference results in a larger curl (Lipponen et al. 2008; Marin Zapata et al. 2013). However, the size of curls might differ even under similar moisture differences. Figure 10 shows the mechanism of the nip curl. When the paper is inside the nip, the moisture migrates from the high temperature region to the low temperature region. However, since the paper is constrained by the rollers, it cannot be deformed due to the change of the moisture content. When the paper is outside of the nip, a larger amount of moisture escapes from the low temperature region, which has a greater moisture content. Therefore, the shrinkage at the low temperature region is larger than that of the high temperature region, which results in the curvature toward the low temperature region. Since the paper is typically considered as a viscoelastic material (Haslach 2000), the time-dependent amount of moisture escaping is important. The strain rate of the paper depends on the change of moisture contents, which can be approximately written as:

$$\frac{\partial \varepsilon}{\partial t} \propto \frac{\partial c_f}{\partial t}, \quad (16)$$

where ε is the strain causing the curl. We calculated the change of the moisture difference in the range between $t = 0.1$ and $t = 0.5$ in order to compare the rate of the moisture escape at the early stage when the paper is outside of the nip. The calculated values are summarized in Table 4. It is clearly observed that the difference increases as the temperature of the heat roller increases. In addition, in terms of the

Table 3 Effect of temperature of rollers inside a fuser on the maximum difference of the moisture content between the surfaces (environment temperature: 30 °C, relative humidity: 85%)

Temperature of the heat roller	Temperature difference between the heat and pressure roller		
	50 °C	65 °C	80 °C
140 °C	0.6631%	0.8496%	1.0103%
170 °C	0.6877%	0.9059%	1.0912%
200 °C	0.6667%	0.8867%	1.1139%

**Fig. 10** Paper curl mechanism in a printer due to moisture transport: **a** moisture inside a paper is distributed uniformly at equilibrium when the paper moves in a fuser, **b** moisture transports from a high temperature region to a low temperature region, **c** when the paper is outside of the fuser, a greater amount

of moisture escapes at the low temperature region than at the high temperature region, **d** paper shrinkage is greater at the low temperature region so the paper is curled toward the low temperature region

Table 4 Changes of the moisture difference at the initial stage after the paper is outside of the nip (environment temperature: 30 °C, relative humidity: 85%)

Temperature of the heat roller	Temperature difference between the heat and pressure roller		
	50 °C	65 °C	80 °C
140 °C	0.4860%	0.6168%	0.7203%
170 °C	0.5524%	0.7037%	0.8577%
200 °C	0.5695%	0.7354%	0.9112%

temperature difference, the tendency is maintained as shown in Table 3. In Fig. 11, the time-dependent variance of the moisture difference at different temperatures of the heat rollers is shown for a temperature difference of 50 °C between the rollers. As the temperature of the heat roller increases, the moisture difference is reduced, indicating faster moisture escape from the low temperature side for higher temperature of the heat roller. This result demonstrates that the paper curl will increase as the temperature of the roller increases.

Although the curl can be simply calculated by moisture expansion from the moisture profiles in analogy to thermal expansion, this simple calculation cannot explain the reversed curl direction, particularly observed in the printing process. Thus, the mechanical model is needed to properly describe the viscoelastic property of paper and the boundary conditions for restraint due to the nip. In the present study, the amount of curl is predicted qualitatively from the moisture differences. The trend predicted from the simulation results agrees well with available data from

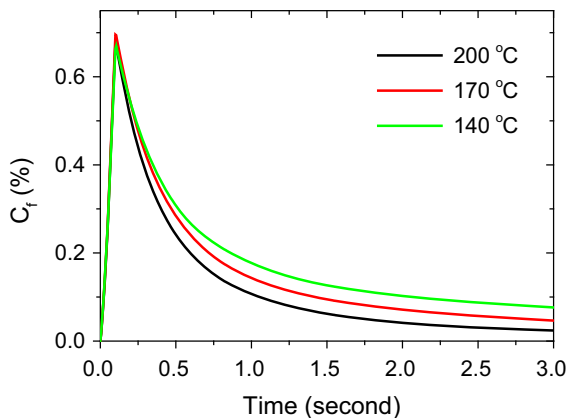


Fig. 11 Change in the difference of moisture content as a function of time with a temperature difference of 50 °C between the rollers (*black* heat roller temperature of 200 °C, *red* heat roller temperature of 170 °C, *green* heat roller temperature of 140 °C). (Color figure online)

experiment, showing the curl becomes larger as the temperature of the heat roller increases (Nonomura et al. 1998; Timofeev et al. 2004).

Conclusions

In this research paper, we derived a mathematical model of moisture transport and heat transport and applied it to a paper sheet that moves through a fusing nip in a printer. We investigated the effect of various parameters that define the conditions of the paper, the environment, and the printer on the moisture transport and distribution along the thickness of the paper. As a result, the mass transport coefficient inside the paper, representing the rate of absorption/desorption between the fibers and pores is an important parameter that determines the order of the gradient of moisture profiles. The parametric study showed that as the values of moisture diffusivity, porosity, and heat conductance between the rollers and paper increase, a greater moisture difference between the high and low temperature regions was observed. In terms of the environmental parameters, relative humidity has a significantly greater effect on the moisture profiles than temperature. In addition, as both the temperature difference between the two rollers in the fusers and the temperature of the heat roller are larger, a larger size of paper curls is expected. The size of curls was predicted

qualitatively based on the maximum moisture difference at the ends of the paper along the thickness. In order to quantitatively calculate the paper curls, a mechanical model should be considered in addition to the moisture transport model. The complete framework, where mechanical, moisture transport, and heat transport models are coupled will be developed in the future for the prediction of the nip curl. By linking the modules for the nip curl and path curl, all of the paper curls in the printing process will be calculated and the simulation results will provide useful data for the engineering design of printers.

Acknowledgments This research was supported by a research grant from S-printing solution and the National Research Foundation of Korea (NRF), funded by the Ministry of Education (NRF-2015R1D1A1A01057759).

References

- Bandyopadhyay A, Radhakrishnan H, Ramarao BV, Chatterjee SG (2000) Moisture sorption response of paper subjected to ramp humidity changes: modeling and experiments. *Ind Eng Chem Res* 39:219–226. doi:[10.1021/ie990279w](https://doi.org/10.1021/ie990279w)
- Bandyopadhyay A, Ramarao BV, Ramaswamy S (2002) Transient moisture diffusion through paperboard materials. *Colloids Surf A* 206:455–467. doi:[10.1016/S0927-7757\(02\)00067-5](https://doi.org/10.1016/S0927-7757(02)00067-5)
- Bedane AH, Xiao H, Eić M (2014) Water vapor adsorption equilibria and mass transport in unmodified and modified cellulose fiber-based materials. *Adsorption* 20:863–874. doi:[10.1007/s10450-014-9628-6](https://doi.org/10.1007/s10450-014-9628-6)
- Bedane AH, Eić M, Farmahini-Farahani M, Xiao H (2016) Theoretical modeling of water vapor transport in cellulose-based materials. *Cellulose* 23:1537–1552. doi:[10.1007/s10570-016-0917-y](https://doi.org/10.1007/s10570-016-0917-y)
- Buck AL (1981) New equations for computing vapor pressure and enhancement factor. *J Appl Meteorol* 20:1527–1532. doi:[10.1175/1520-0450\(1981\)020<1527:nefcvp>2.0.co;2](https://doi.org/10.1175/1520-0450(1981)020<1527:nefcvp>2.0.co;2)
- Carlsson L (1981) Out-of-plane hygroinstability of multi-ply paperboard. *Fibre Sci Technol* 14:201–212. doi:[10.1016/0015-0568\(81\)90012-9](https://doi.org/10.1016/0015-0568(81)90012-9)
- Coffin DW, Lif JO, Fellers C (2004) Tensile and ultrasonic stiffness of paper at different moistures—a clarification of the differences. *Nord Pulp Pap Res J* 19:257–263
- Fan J, Wen X (2002) Modeling heat and moisture transfer through fibrous insulation with phase change and mobile condensates. *Int J Heat Mass Transf* 45:4045–4055. doi:[10.1016/S0017-9310\(02\)00114-X](https://doi.org/10.1016/S0017-9310(02)00114-X)
- Gupta H, Chatterjee SG (2003a) Parallel diffusion of moisture in paper. Part 1: steady-state conditions. *Ind Eng Chem Res* 42:6582–6592. doi:[10.1021/ie030413j](https://doi.org/10.1021/ie030413j)
- Gupta H, Chatterjee SG (2003b) Parallel diffusion of moisture in paper. Part 2: transient conditions. *Ind Eng Chem Res* 42:6593–6600. doi:[10.1021/ie030414b](https://doi.org/10.1021/ie030414b)

- Habeger CC, Coffin DW (2000) The role of stress concentrations in accelerated creep and sorption-induced physical aging JPPS. *J Pulp Pap Sci* 26:145–157
- Habeger CC, Coffin DW, Hojjatie B (2001) Influence of humidity cycling parameters on the moisture-accelerated creep of polymeric fibers. *J Polym Sci Part B Polym Phys* 39:2048–2062. doi:[10.1002/polb.1180](https://doi.org/10.1002/polb.1180)
- Haslach HW (2000) The moisture and rate-dependent mechanical properties of paper: a review. *Mech Time Depend Mater* 4:169–210. doi:[10.1023/a:1009833415827](https://doi.org/10.1023/a:1009833415827)
- Huang H, Ye C, Sun W (2007) Moisture transport in fibrous clothing assemblies. *J Eng Math* 61:35–54. doi:[10.1007/s10665-007-9201-3](https://doi.org/10.1007/s10665-007-9201-3)
- Land C, Wahlström T, Stolpe L, Beghello L (2010) Plastic strain of moisture streaks at different moisture contents. *Nord Pulp Pap Res J* 25:481–487
- Larsson PA, Wågberg L (2010) Diffusion-induced dimensional changes in papers and fibrillar films: influence of hydrophobicity and fibre-wall cross-linking. *Cellulose* 17:891–901. doi:[10.1007/s10570-010-9433-7](https://doi.org/10.1007/s10570-010-9433-7)
- Leisen J, Hojjatie B, Coffin DW, Lavrykov SA, Ramarao BV, Beckham HW (2002) Through-plane diffusion of moisture in paper detected by magnetic resonance imaging. *Ind Eng Chem Res* 41:6555–6565. doi:[10.1021/ie0204686](https://doi.org/10.1021/ie0204686)
- Linville E, Östlund S (2014) The combined effects of moisture and temperature on the mechanical response of paper. *Exp Mech* 54:1329–1341. doi:[10.1007/s11340-014-9898-7](https://doi.org/10.1007/s11340-014-9898-7)
- Linville E, Östlund S (2016) Parametric study of hydroforming of paper materials using the explicit finite element method with a moisture-dependent and temperature-dependent constitutive model. *Packag Technol Sci* 29:145–160. doi:[10.1002/pts.2193](https://doi.org/10.1002/pts.2193)
- Lipponen P, Leppänen T, Kouko J, Hämäläinen J (2008) Elastoplastic approach for paper cockling phenomenon: on the importance of moisture gradient. *Int J Solids Struct* 45:3596–3609. doi:[10.1016/j.ijsolstr.2008.02.017](https://doi.org/10.1016/j.ijsolstr.2008.02.017)
- Marin Zapata PA, Fransen M, ten Thije BJ, Saes L (2013) Coupled heat and moisture transport in paper with application to a warm print surface. *Appl Math Model* 37:7273–7286. doi:[10.1016/j.apm.2013.02.032](https://doi.org/10.1016/j.apm.2013.02.032)
- Menart E, De Bruin G, Strlič M (2011) Dose–response functions for historic paper. *Polym Degrad Stab* 96:2029–2039. doi:[10.1016/j.polymdegradstab.2011.09.002](https://doi.org/10.1016/j.polymdegradstab.2011.09.002)
- Neagu RC, Gamstedt EK, Lindström M (2005) Influence of wood-fibre hygroexpansion on the dimensional instability of fibre mats and composites. *Compos Part A Appl Sci Manuf* 36:772–788. doi:[10.1016/j.compositesa.2004.10.023](https://doi.org/10.1016/j.compositesa.2004.10.023)
- Noboa HL, Seyed-Yagoobi J (2001) Thermal contact conductance of a coated paper/metal interface. *Drying Technol* 19:1125–1135. doi:[10.1081/drt-100104809](https://doi.org/10.1081/drt-100104809)
- Nonomura F, Abe Y, Takeuchi N (1998) A study on the curling behaviour of paper resulting from heatroller heating (I) Japan. *Tappi J* 52:535–542. doi:[10.2524/jtappij.52.535](https://doi.org/10.2524/jtappij.52.535)
- Parker ME, Bronlund JE, Mawson AJ (2006) Moisture sorption isotherms for paper and paperboard in food chain conditions. *Packag Technol Sci* 19:193–209. doi:[10.1002/pts.719](https://doi.org/10.1002/pts.719)
- Quirijns EJ, van Boxtel AJB, van Loon WKP, van Straten G (2005) Sorption isotherms GAB parameters and isosteric heat of sorption. *J Sci Food Agric* 85:1805–1814. doi:[10.1002/jsfa.2140](https://doi.org/10.1002/jsfa.2140)
- Ramarao BV, Massoquete A, Lavrykov S, Ramaswamy S (2003) Moisture diffusion inside paper materials in the hygroscopic range and characteristics of diffusivity parameters. *Dry Technol* 21:2007–2056. doi:[10.1081/drt-120027044](https://doi.org/10.1081/drt-120027044)
- Sáez AE, Otero CJ, Rusinek I (1989) The effective homogeneous behavior of heterogeneous porous media. *Transp Porous Media* 4:213–238. doi:[10.1007/bf00138037](https://doi.org/10.1007/bf00138037)
- Salmen NL, Back EL (1980) Moisture-dependent thermal softening of paper, evaluated by its elastic modulus. *Tappi* 63:117–120
- Timofeev O, Keranen J, Kiiskinen H, Kiuru J, Tanaka A (2004) Temperature measurements and simulations inside a paper in a fuser nip. In: *Proceedings of the 14th international drying symposium B*, pp 1249–1254